

The stopping of low energy ions in reactions of astrophysical interest

Carlos A. BERTULANI

National Superconducting Cyclotron Laboratory, Michigan State University, East Lansing, MI 48824, USA

The velocity dependence of the stopping power of swift protons and deuterons in low energy collisions with hydrogen and helium gas targets is investigated with the numerical solution of the time-dependent Schrödinger coupled-channels equations using molecular orbital wavefunctions. At low projectile energies the stopping is mainly due to nuclear stopping, charge exchange of the electron, and excitation of the lowest levels in the target. The second and third mechanisms dominate at $E < 200$ eV. At lower energies it is also shown that a threshold effect is responsible for a quick drop of the energy loss. This investigation sheds more light on the long standing electron screening problem in fusion reactions of astrophysical interest.

Nuclear fusion reactions proceed in stars at extremely low energies, e.g., of the order of 10 keV in our sun.^{1),2)} At such low energies it is extremely difficult to measure the cross sections for charged particles at laboratory conditions due to the large Coulomb barrier. One often uses a theoretical model to extrapolate the experimental data to the low-energy region. Such extrapolations are sometimes far from reliable, due to unknown features of the low-energy region. E.g., there might exist unknown resonances along the extrapolation, or even some simple effect which one was not aware of before. One of these effects is the laboratory atomic screening of fusion reactions.^{3),4)} It is well known that the laboratory measurements of low energy fusion reactions are strongly influenced by the presence of the atomic electrons. This effect has to be corrected for in order to relate the fusion cross sections measured in the laboratory with those at the stellar environment. One has observed experimentally a large discrepancy between the experimental data and the best models available to treat the screening effect by the electrons in the target nuclei.⁵⁾ The screening effect arises because as the projectile nucleus penetrates the electronic cloud of the target the electrons become more bound and the projectile energy increases by energy conservation. Since fusion cross sections increase strongly with the projectile's energy, this tiny amount of energy gain (of order of 10-100 eV) leads to a large effect on the measured cross sections. However, in order to explain the experimental data it is necessary an extra-amount of energy about twice the expected theoretical value.⁵⁾

In order to extract the fusion cross sections from experiment one needs to correct for the energy loss in the target to assign the correct projectile energy value for the reaction. The authors in refs.^{6),7)} have shown that a possible solution to the long standing discrepancy between theory and experiment for the reaction ${}^3\text{He}(d, p){}^4\text{He}$ could be obtained if the projectile energy loss by electronic excitations and charge exchange with the target atoms would be smaller than previously assumed in the

experimental data analysis. There have been indeed a few experiments in which evidences of smaller than expected electronic stopping power were reported (see, e.g. ref.⁸⁾). Other reactions of astrophysical interest (e.g., those listed in by Rolfs and collaborators^{3),4)}) should also be corrected for this effect. Whereas at higher energies the stopping is mainly due to the ionization of the target electrons, at the astrophysical energies it is mainly due to excitations of the lowest levels, charge-exchange between the target and the projectile, and the nuclear stopping power.

The static two-center p+H system has been solved by Edward Teller in 1930.⁹⁾ He showed that as the distance between the protons decreases the hydrogen orbitals split into two or more orbitals, depending on its degeneracy in the two-center system. Analogous problems are well known in quantum systems. For example, take two identical potential wells at a certain distance. For large distances the states in one well are degenerated with the states in the other potential well. As they approach this degeneracy is lifted due to the influence of barrier tunnelling. Thus, the lowest energy state of hydrogen, 1s, splits into the 1σ and the $2p\sigma$ states as the protons approach each other. The 1σ state is space symmetrical, while the $2p\sigma$ state is antisymmetric. As the proton separation distance decreases their respective energies decrease. At $R \simeq 1 \text{ \AA}$ the energy of the $2p\sigma$ state starts to increase again, while the energy of the 1σ state continues to decrease. For proton distances much smaller than 1 \AA the 1σ and the $2p\sigma$ energies correspond to those of the first and second states of the He atom, respectively.⁹⁾

The full time-dependent wavefunction for the system can be expanded in terms of two-center states, $\phi_n(t)$, governed by the Schrödinger's equation. For the p+H system and at very low proton energies ($E_p \lesssim 1 \text{ keV}$) it is fair to assume that only the low-lying states are involved in the electronic dynamics. Only at proton energies of order of 25 keV the proton velocity is comparable to the electron velocity, $v_e \simeq \alpha c$. Thus, the evolution of the system is almost adiabatic at $E_p \lesssim 10 \text{ keV}$. The higher states require too much excitation energy and belong to different degeneracy multiplets. The initial electronic wavefunction is a clear superposition of 1σ and $2p\sigma$ two-center states. One thus expects that only these states are relevant for the calculation. In fact, at these energies the population of the 2p atomic state in charge exchange is much less than the population of the 1s atomic state. These assumptions are well supported by the calculations of Grande and Schwietz,¹⁰⁾ who have used a dynamical approach based on target-centered wavefunctions. In their approach one has to include a great amount of target-centered states in order to represent well the strong distortion of the wavefunction as the projectile closes in the target. We also have assumed that the proton follows a classical trajectory determined by an impact parameter b .

If one includes only the two lowest energy molecular states in the p+H system, Schrödinger's equation becomes¹¹⁾

$$i\hbar \frac{d}{dt} \begin{pmatrix} a_+ \\ a_- \end{pmatrix} = \begin{pmatrix} V_+ + E_0 & iW \\ iW & V_- + E_0 \end{pmatrix} \begin{pmatrix} a_+ \\ a_- \end{pmatrix}, \quad (0-1)$$

where the indices + and - refer to the 1σ and $2p\sigma$ states, respectively, $E_0 = -13.6 \text{ eV}$, $V_{\pm}(t) = E_{\pm}(t) - E_0$, and $W(t)$ is the residual potential.¹¹⁾ We use the

formalism of Teller⁹⁾ to calculate the wavefunctions $\Psi_{\pm}(R)$ at different inter-proton distances, $R(t)$, corresponding to a particular time t . The static Schrödinger equation is solved in elliptical coordinates. This yields two coupled differential equations which can be solved by expanding the solutions in Taylor series. A set of recurrence relations is obtained for the expansion coefficients when the boundary conditions are used. The energies $E_{1s\sigma}(R)$ and $E_{2p\sigma}(R)$ are obtained by adjusting the constant which separates the two coupled equations¹¹⁾ to its correct matching value.

It was further shown in ref.¹¹⁾ that the potentials $V_{\pm}(t)$ extend much farther out than $W(t)$. Moreover, as E_p decreases the potential W decreases faster than the projectile's velocity, v_p . At $E_p \simeq 100$ eV the potential W loses its relevance as compared to V_{\pm} , which have no dependence on v_p . When one sets $W = 0$ in eq. (0.1), the equations decouple and it is straightforward to show that the exchange probability is given by

$$P_{exch} = \frac{1}{2} + \frac{1}{2} \cos \left\{ \frac{1}{\hbar} \int_{-\infty}^{\infty} [E_-(t) - E_+(t)] dt \right\}. \quad (0.2)$$

At $E_p = 10$ keV there is an appreciable difference between the full calculation and the approximation (0.2). But, for $E_p = 100$ eV the results are practically equal, except for very small impact parameters at which the potential W still has an effect.

The exchange probability is not constant at small impact parameters, but oscillates wildly around 0.5, specially for low projectile energies. One might naively assume that because the collision is almost adiabatic, the system loses memory of to which nucleus the electron is bound after the collision. Thus, for small impact parameters one would expect a 50% probability of finding the electron in one of the nuclei at $t = \infty$. However, this is not what happens. From eq. (0.2) we see that minima of the probability occur for impact parameters satisfying the relation $\int_{-\infty}^{\infty} [E_-(t) - E_+(t)] dt = 2\pi\hbar(n + 1/2)$, $n = 0, 1, 2, \dots, N$.

This relation looks familiar, of course. It simply states that the interference between the $1s\sigma$ and the $2p\sigma$ states induces oscillations in the exchange probability. The electron tunnels back and forth between the projectile and the target during the ingoing and the outgoing part of the trajectory. When the interaction time is an exact multiple of the oscillation time, a minimum in the exchange probability occurs. The average probability over the smaller impact parameters is indeed 0.5. As the impact parameter decreases from infinity, the first maximum in the exchange probability indicates the beginning of the region of strong exchange probability. At low proton energies this starts at $b \simeq 3$ Å. The size of the hydrogen atom is about 0.5 Å and thus the electron travels in a forbidden region (tunnels) of about 2 Å from the target to the projectile. This is possible because of the strong interference between the $1s\sigma$ and the $2p\sigma$ states, which for some trajectories satisfy the quantum relation above.

To obtain the stopping power we need the total cross section for charge exchange, $\sigma = 2\pi \int P_{exch} b db$. For $E_p \rightarrow 0$, the charge exchange cross section becomes the constant value $\sigma(E_p = 0) = 37.88 \times 10^{-16}$ cm². This happens because, when $E_p \rightarrow 0$ and as the projectile nears the targets, the increasing electron binding in the two-center system acts as a push in the relative motion energy to compensate for

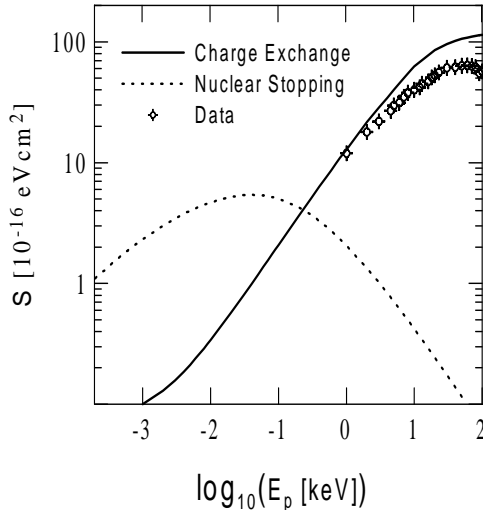


Fig. 1. The stopping cross section of protons on H-targets. The dotted line in gives the energy transfer by means of nuclear stopping, while the solid line are our results for the charge-exchange stopping mechanism. The data points are from the tabulation of Andersen and Ziegler.¹³⁾

energy conservation. The average result is that the cross section for charge exchange becomes approximately constant for projectile energies of tens of eV and below.

In figure 1 we show the stopping cross section of the proton. The stopping cross section is defined as $S = \sum_i \Delta E_i \sigma_i$, where ΔE_i is the energy loss of the projectile in a process denoted by i . The stopping power, $S_P = dE/dx$, the energy loss per unit length of the target material, is related to the stopping cross section by $S = S_P/N$, where N is the atomic density of the material. In the charge exchange mechanism the electron is transferred to the ground state of the projectile and the energy transfer is given by $\Delta E = m_e v_p^2/2$, where v_p is the projectile velocity. Assuming that there are a few free electrons in the material (e.g., in a hydrogen gas) only one more stopping mechanism at very low energies should be considered: the nuclear stopping power. This is simply the elastic scattering of the projectile off the target nuclei. The projectile energy is partially transferred to the recoil energy of the target atom. The stopping cross section for this mechanism has been extensively studied in ref.¹²⁾ The nuclear stopping includes the effect of the electron screening of the nuclear charges.

The dotted line in figure 1 gives the energy transfer by means of nuclear stopping, while the solid line are our results for the charge-exchange stopping mechanism. The data points are from the tabulation of Andersen and Ziegler.¹³⁾ We see that the nuclear stopping dominates at the lowest energies, while the charge-exchange stopping is larger for proton energies greater than 200 eV. Since we neglect the difference between molecular and atomic hydrogen targets, there is a limitation to compare our results with the experimental data. But, the order of magnitude agreement is very good in view of our simplifying assumptions. We do not consider the change of the charge state of the protons as they penetrate the target material. The exchange

mechanism transforms the protons into H atoms. These again interact with the target atoms. They can lose their electron again by transfer to the 1s state of the target.¹⁰⁾

The best fit to our calculation for the stopping power for proton energies in the range 100 eV - 1 keV yields $S \sim v_p^{1.35}$. This contrasts with the extrapolation $S \sim v_p$, based on the Andersen-Ziegler tables.

Let us now consider the systems $p+^4\text{He}$ and $d+^3\text{He}$. The situation is more complicated because of the electron-electron interaction. The atomic wavefunctions, $\phi_\mu = \sum_j c_{j\mu} \phi_j^{Slat}$, are constructed as a linear combination of Slater-type orbitals (STO)¹⁴⁾ of the form $\phi_n^{Slat} = N r^{n-1} \exp(-\zeta r) Y_{lm}(\hat{\mathbf{r}})$, where the Slater coefficients n and ζ are chosen to best approximate the exact atomic wavefunctions (see, e.g. ref.¹⁴⁾). The molecular orbital wavefunctions for the $p + \text{He}$ system, are obtained with the ϕ_μ 's chosen so that half of the STO's are centered on the proton (A) and the other half are centered on the helium nucleus (B). The total wavefunction for the two-electron system is finally written as a Slater determinant of the molecular orbital wavefunctions. Configuration-interaction with double excitation configurations were included in the calculation,¹⁵⁾ with the coefficients n and the Slater parameters ζ chosen in a variational method to obtain the lowest energy states of the system.

Using these conditions and variation method, one obtains the Hartree-Fock equations for the electronic states. Solving the Hartree-Fock equations one obtains the coefficients c_{ij} which give the proper linear combination of atomic orbitals to form the molecular orbital.

In figure 2 we show the intersection points of the states with same symmetry in the $\text{H}^+ + \text{He}$ system. In a fast collision these states would cross (diabatic collisions), whereas in collisions at very low energies (adiabatic collisions) they obey the von Neumann-Wigner non-crossing rule.

In the dynamical case the full time-dependent wavefunction for the system can be expanded in terms of two-center states, with expansion coefficients $a_n(t)$. The dynamical evolution of the $\text{H} + \text{He}$ system is calculated using the same approach as described in ref.¹¹⁾ The solutions are obtained starting from initial internuclear distance of 15 a.u. for the incoming trajectory and stopped at the same value for the outgoing trajectory. The probability for the capture in the proton is obtained by a projection of the final wavefunction into the wavefunctions of the 1s, 2s and 2p states of the hydrogen atom.

A similar situation occurs for $p + \text{He}$ collisions for the electron capture probability by the proton at a few keV bombarding energy. There will be oscillations due to the electron exchange between the ground state of the hydrogen and the first excited state in He (1s2s). But, in contrast to the $\text{H}^+ + \text{H}$ system, the oscillations are strongly damped. Following the work of Lichten¹⁶⁾ we interpret this damping effect as due to the interference between the participant states and a band of states of average energy $\langle E_a \rangle$ and width 2Γ , as seen in figure 2. The important regions where the diabatic level cross occurs is shown in figure 2 inside the encircled areas. The damping mechanism is best understood using the Landau-Zener theory for level crossing. At the crossing there is a particular probability $(1 - P)$ of an adiabatic transition where

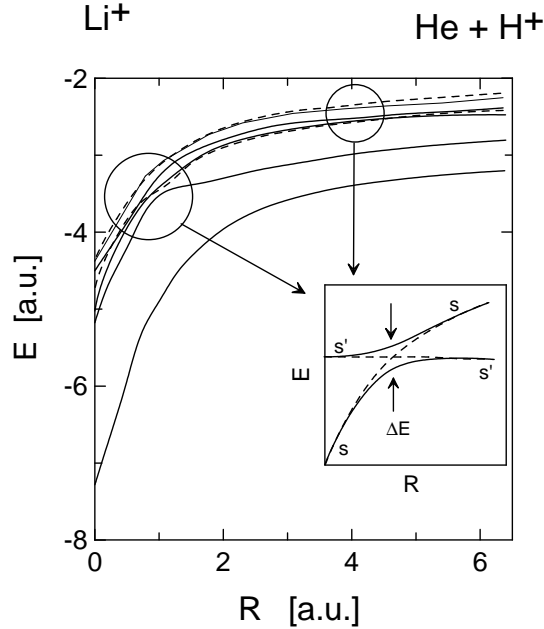


Fig. 2. Adiabatic energies (1 a.u. of energy = 27.2 eV, 1 a.u. of length = 0.53 Å) for the electronic orbitals for the $(\text{H-He})^+$ system as a function of the internuclear separation. As the atoms approach each other slowly curves of same symmetry repel each other. A transition between states s and s' can occur in a slow collision. In a fast collision a diabatic transition, with the states crossing each other, will occur. This is shown in the inset.

P is given by the Landau-Zener formula

$$P_{exch} = \exp \left[\frac{2\pi H_{ss'}^2}{v(d/dR)(E_s - E_{s'})} \right] \quad (0.3)$$

where v is the collision velocity and $H_{ss'}$ is the off-diagonal matrix element connecting states s and s' . The oscillatory behavior of the exchange probability is due to the many level transitions at the crossing. The interference with the neighboring states introduces a damping in the charge exchange probability, i.e.

$$P_{exch}(b, t) \simeq \cos^2 \left(\frac{\langle E_a \rangle b}{v} \right) \exp \left[-\frac{2\pi \Gamma^2 b}{v \langle E_a \rangle} \right],$$

where $\langle E_a \rangle \simeq 1$ a.u. is the average separation energy between the 0Σ level and the bunch of higher energy levels shown in figure 2. The exponential damping factor agrees with the numerical calculations if one uses $\Gamma \simeq 5$ eV, which agrees with the energy interval of the band of states shown in figure 2.

At very low energies the only possibility that the electron is captured by the proton is if there is a transition $1s^2(^1S_0) \rightarrow 1s2s(^3S)$ in the helium target. Only in this case the energy of one of the electrons in helium roughly matches the electronic energy of the ground state in H. This resonant transfer effect is responsible for the large capture cross sections. When this transition is not possible the electrons

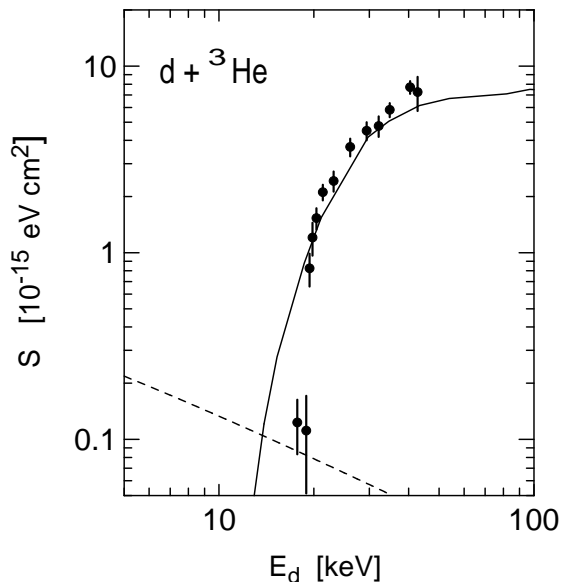


Fig. 3. Energy loss of deuterons in ^3He gas as a function of deuteron energy. Data are from ref.¹⁷⁾ The solid curve is the calculation for the electronic stopping power, while the dashed curve shows the nuclear stopping.

prefer to stay in the helium target, as the energy of the whole system is lowest in this case. Another possible mechanism for the stopping is the excitation of the helium atom by the transition $1s^2(^1S_0) \rightarrow 1s2s(^3S)$. Thus, there must be a direct relationship between the energy transfer to the transition $1s^2(^1S_0) \rightarrow 1s2s(^3S)$ and the minimum projectile energy which enables electronic changes. Ref.¹⁷⁾ reported for the first time this effect, named by threshold energy, which can be understood as follows. The momentum transfer in the projectile-target collision, Δq , is related to the energy transfer to the electrons by $\Delta q = \Delta E/v$, where v is the projectile velocity. In order that this momentum transfer absorbed by the electron, induces an atomic transition, it is necessary that $\hbar^2 \Delta q^2 / 2m_e \sim \Delta E$. Solving these equations for the projectile energy one finds

$$E_p^{thres} \sim \frac{m_p}{4m_e} \Delta E. \quad (0.4)$$

This is the threshold energy for atomic excitations and/or charge exchange. If the projectile energy is smaller than this value, no stopping should occur. The energy for transition $1s^2(^1S_0) \rightarrow 1s2s(^3S)$ in He is $\Delta E = 18.7$ eV. Thus, for p + He collisions, the threshold energy is $E_p^{thres} \sim 9$ keV.

Figure 3 shows the energy loss of deuterons in ^3He gas as a function of deuteron energy. The data are from ref.¹⁷⁾ The solid curve is the numerical calculation for the electronic stopping power, while the dashed curve shows the nuclear stopping. As discussed in ref.¹⁷⁾ the threshold deuteron energy in this reaction is of the order of 18 keV, which agrees with the estimate based on eq. 0.4. However, the numerical

calculations based on the electronic stopping (solid curve of fig. 3) indicate a lower threshold energy for this system. Nonetheless, the agreement with the experimental data is very good for $E_d > 20$ keV. The threshold effect is one more indication that the extrapolation $S \sim v$, based on the Andersen-Ziegler tables is not applicable to very low energies.

The steep rise of the fusion cross sections at astrophysical energies amplifies all effects leading to a slight modification of the projectile energy.¹⁸⁾ The results presented here show that the stopping mechanism does not follow a universal pattern for all systems. The threshold effect reported in ref.¹⁷⁾ is indeed responsible for a rapid decrease of the electronic stopping at low energies. It will occur whenever the charge-exchange mechanism and the excitation of the first electronic state in the target involve approximately the same energy. However, the drop of the electronic stopping is not as sharp as expected from the simple classical arguments given by eq. 0-4.

The experiments on astrophysical fusion reactions have shown that the screening effect is much larger than expected by theory. The solution to this problem might be indeed the smaller stopping power, due to a steeper slope at low energies induced, e.g. by the threshold mechanism. This calls for improved theoretical studies of the energy loss of ions at extremely low energies of and for their independent experimental verification. The present situation is highly disturbing because if we cannot explain the laboratory screening effect, most likely we cannot explain it in stellar environments.

References

- 1) D.D. Clayton, *Principles of Stellar Evolution and Nucleosynthesis*, McGraw-Hill, New York, 1968
- 2) C. Rolfs and W.S. Rodney, *Cauldrons in the Cosmos*, Chicago Press, Chicago, 1988
- 3) H.J. Assenbaum, K. Langanke, and C. Rolfs, *Z. Phys.* **A327**, 461 (1987)
- 4) E. Somorjai and C. Rolfs, *Nucl. Instrum. Meth.* **B99**, 297 (1995)
- 5) C. Rolfs, *Prog. Part. Nucl. Phys.* **46**, 23 (2001)
- 6) K. Langanke, T.D. Shoppa, C.A. Barnes and C. Rolfs, *Phys. Lett.* **B369**, 211 (1996)
- 7) J.M. Bang, L.S. Ferreira, E. Maglione, and J.M. Hansteen, *Phys. Rev.* **C53**, R18 (1996)
- 8) R. Golser and D. Semrad, *Phys. Rev. Lett.* **14**, 1831 (1991)
- 9) E. Teller, *Z. Physik*, **61**, 458 (1930)
- 10) P.L. Grande and G. Schiwietz, *Phys. Rev.* **A47** (1993) 1119; *Phys. Rev.* **A58**, 3796 (1998); *Nucl. Inst. Meth.* **B153**, 1 (1999)
- 11) C.A. Bertulani and D.T. de Paula, *Phys. Rev.* **C 62**, 045802 (2000)
- 12) J.F. Ziegler, J.P. Biersack and U. Littmark, *The stopping and range of ions in matter*, Vol. 1, Pergamon Press, New York (1985)
- 13) H. Andersen and J.F. Ziegler, *The stopping and ranges of ions in matter*, Vol. 3, Pergamon press, New York (1977)
- 14) I.N. Levine, *Quantum Chemistry*, 5th ed., Prentice Hall (2000)
- 15) C.A. Bertulani, nucl-th/0401002
- 16) W. Lichten, *Phys. Rev.* **131** (1963) 229
- 17) A. Formicola et al., *Eur. Phys. J.* **A8**, 443 (2000)
- 18) A. B. Balantekin, C. A. Bertulani, M. S. Hussein, *Nucl. Phys.* **A627**, 324 (1997)